Micro Aerial Vehicle (MAV): An Aerodynamics Optimized Design

by

Wong Peck Koon

Dissertation submitted in partial fulfillment of
the requirements for the
Bachelor of Engineering (Hons)
(Mechanical Engineering)

JUNE 2009

Universiti Teknologi PETRONAS
Bandar Seri Iskandar
31750 Tronoh
Perak Darul Ridzuan

CERTIFICATION OF APPROVAL

Micro Aerial Vehicle (MAV): An Aerodynamics Optimized Design

by

Wong Peck Koon

A project dissertation submitted to the
Mechanical Engineering Programme
Universiti Teknologi PETRONAS
in partial fulfillment of the requirement for the
BACHELOR OF ENGINEERING (Hons)
(MECHANICAL ENGINEERING)

Approved by,

_____
(Dr Ahmed Maher Said Ali)
Project Supervisor

UNIVERSITI TEKNOLOGI PETRONAS

TRONOH, PERAK

JUNE 2009

CERTIFICATION OF ORIGINALITY

This is to certify that I am responsible for the work submitted in this project, that the original work is my own except as specified in the references and acknowledgements, and that the original work contained herein have not been undertaken or done by unspecified sources or persons.

_____

(Wong Peck Koon)

ABSTRACT

Unmanned Aerial Vehicles (UAV) have played more and more important roles, not only in military, but also in civil applications nowadays. UAV differs than normal aircraft due to different aerodynamic characteristics. Studying UAV aerodynamic leads to an optimized successful design. Micro Aerial Vehicles (MAV) are smaller versions of UAV, with lower Reynolds number and lower weight.

The purpose of this project is to perform a technical study on aerodynamic characteristic of Micro Aerial Vehicles (MAV) at different Angles of Attack (AOA) and with varying wing shapes and areas if necessary. The background study consists of understanding of Unmanned Aerial Vehicles (UAV), Micro Aerial Vehicles (MAV), forces of flight, lift and drag coefficient. The literature review summarizes research of UAV problems since the invention, optimization of aerodynamic characteristic and numerical testing carried out on aircraft. The methodology planned consists of numerical testing, which is performed by using Computational Fluid Dynamic simulation using the commercial code FLUENT. MAV Design 2 shows improved $C_{L,}$ Lift Coefficient compared to MAV Design 1. The finer meshing shows more accurate result as compared to coarser and uniform meshing. For MAV Design 2 and MAV Design 3, as Angle of Attack increases, C_L increases. This shows the same C_L versus Angles of Attack relation as the published data. Hence the results show reasonable predictions of lift and drag coefficients.

ACKNOWLEDGEMENTS

Throughout this whole duration of this project, I've learnt a lot and gained priceless experiences. I would like to acknowledge the following people for their help, advice, support and encouragement throughout this duration. Without them, this project could never have been done with so much content.

I could never have come so far without the constant supervision and support of my supervisor, Dr Ahmed. Thank you for your constant guidance, advice and encouragement throughout this whole year. Your help is greatly appreciated.

To Graduate Assistances, thank you for your guidance along the time, to help me out on the project. To Lab Technician, thank you for your help especially when I need to use computers in laboratory. You always try your best to help me.

To my friends both from UTP and elsewhere, thanks for always being there for me. Thank you for sharing the knowledge with me.

Finally, to all who have helped me in one way or another, thank you.

TABLE OF CONTENTS

LIST OF FIGURES

LIST OF TABLES

CHAPTER 1

INTRODUCTION

1.1 BACKGROUND STUDY

Unmanned Aerial Vehicles (UAV) history started at early 19th century. Researches and developments have been rapidly carried out in United States, Iraq, Japan, China, Australia and others. Micro Aerial Vehicles (MAV) development started rapidly in 1996.

1.1.1 Unmanned Aerial Vehicles (UAV)

The term Unmanned Aerial Vehicles (UAV) came into general use in early 1990s to describe robotic aircraft and replaced the term Remotely Piloted Vehicle (RPV). The Department of Defense Dictionary defines a UAV as a powered, aerial vehicle that doesn't carry a human operator, uses aerodynamic forces to provide vehicle lift, can fly autonomously or be piloted remotely, can be expandable or recoverable, and can carry a lethal or non-lethal payload. Ballistic or semi-ballistic vehicles, cruise missiles and artillery projectiles are not considered as UAV [1].

Different UAV can be different in terms of sizes, shapes and configurations, depending on the design. The famous types of medium sized UAV are Luna, Hunter, X-sight and Pioneer.

UAV is important in military and civil applications such as fire fighting, police observation and reconnaissance support in natural disaster. The UAV functions can be mainly divided into six, which are Target and decoy, Reconnaissance, Combat, Logistic, Research and Development, Civil and Commercial.

1.1.2 Micro Aerial Vehicles (MAV)

Micro Aerial Vehicles (MAV) are aircrafts that are designed as small as possible for special and limited duration missions. The size of MAV is small. Hence MAV flies at very low speed. The range of speed is found to be from 24 to 64 km/h (or 15 to 40mph). The range of Reynolds number is found to be from approximately $5x10^4$ to $2x10^5$. The various types of MAV that exist until now are fixed or rigid wing, flexible wing and adaptive wing.

MAV is important in surveillance, detection and communication. Small sensors may be installed in MAV for sensing of biological agents, chemical compounds and nuclear materials. To improve communication, MAV is used in urban area. MAV is also used in hostage rescue and counter drug operation [2] and [3].

1.1.3 Forces of flight

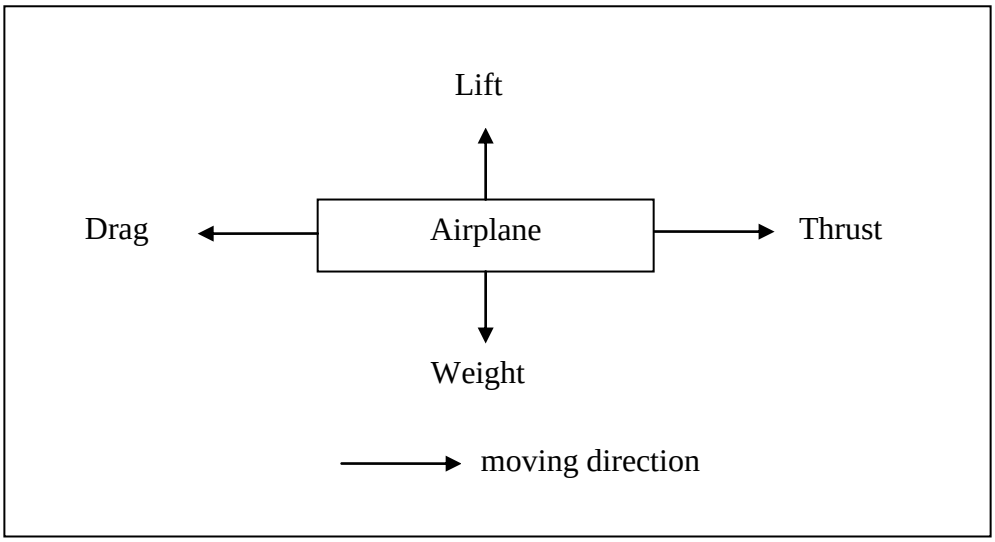

FIGURE 1.1: Forces Acting on an Airplane

Forces of flight include lift at the upward direction, drag at the opposite direction of flight motion, thrust at flight motion direction, and weight at the direction of gravity. This can be shown in Figure 1.1.

Lift and drag are categorized as aerodynamic forces. Lift is the upward force of a flight, which is important to maintain a flight on air. Lift is created when the pressure difference is lower at the upper surface as compared to the lower surface of the plane. Lift can be increased by increasing the plane's forward speed or by increasing the plane's angle of attack. Drag is the resistance created by air.

1.1.4 Lift and Drag Coefficient

In aerodynamic, the important non-dimensional quantities are Reynolds number and Mach number. Reynolds number is the ratio of inertial and viscous force. Mach number is the ratio of airspeed to speed of sound.

In an aircraft configuration, the force coefficient (lift or drag coefficient) is shown to be depended on Mach number (M), Reynolds number (Re), angles of attack (α) and geometry shape of the aircraft (t). The relationship between force coefficient and those parameters mentioned is shown in the following equations [4].

$$C_L = C_L (\alpha , Re, M, t)$$

$$C_D = C_D (\alpha , Re, M, t)$$

The lift coefficient can be represents by the following equations [5]:

$$C_L = \frac{F_L}{0.5\rho V^2 S}$$

where F_L=lift force, ρ = air density, V= relative speed between body and free-stream velocity, S= reference area

$$C_L = 2 \Pi \alpha$$

where α = angle of attack

The lift coefficient can be represents by the following equations [5]:

$$C_D = \frac{F_D}{0.5\rho V^2 S}$$

where F_D= drag force, ρ = air density , V= relative speed between body and free-stream velocity, A= reference area

From the lift coefficient equation, it shows that lift coefficient increases with the angle of attack. However, after a certain maximum value, lift coefficient will decrease with the increases of angle of attack. This condition is called stall. Stall occurs because of the onset of separation flow on the top of airfoil. The lift, drag coefficient and angle of attack graph is shown in Figure 1.2 [5].

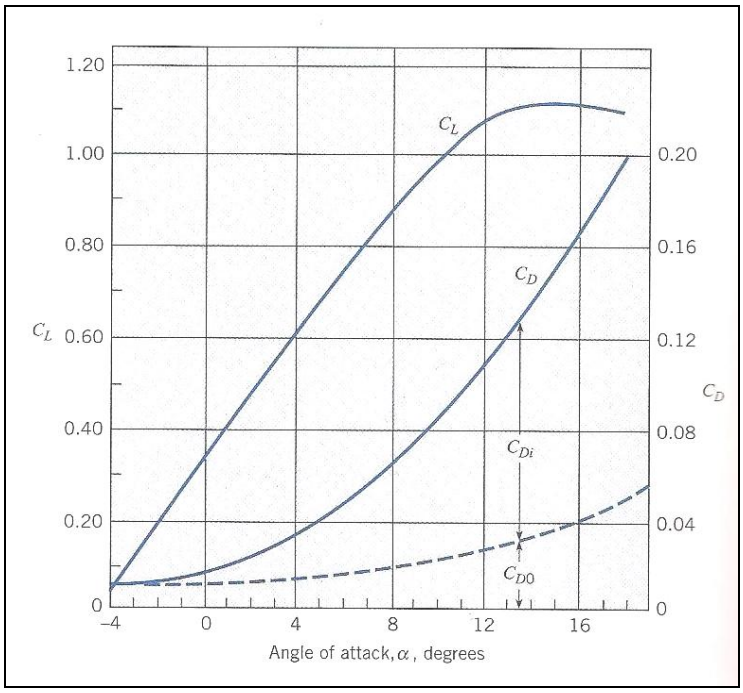

FIGURE 1.2: Coefficient of lift and drag with an aspect ratio of 5 [5]

1.2 PROBLEM STATEMENT

Although a lot of research has been carried out on the aerodynamics of different airfoils, very little information is available on the aerodynamics of low aspect ratio wings. Moreover, low speed of MAV results in low Reynolds number, which then increases viscous drag.

1.3 OBJECTIVES

The objective of this project is to design an aerodynamic optimised MAV, with high lift and low drag.

1.4 SCOPE OF STUDY

The scopes of study include the understanding on the basic principle of flight. Basic principle of flight includes forces acting on an airplane. Other project scopes include understanding on Unmanned Aerial Vehicles (UAV) and Micro Aerial Vehicles (MAV) aerodynamic characteristic and also Computational Fluid Dynamic (CFD) code.

The scopes of study are summarized as following:

i) Understanding fundamental of flight
ii) Studying aerodynamic characteristics of Unmanned Aerial Vehicles (UAV) and Micro Aerial Vehicles (MAV)
iii) Studying Computational Fluid Dynamic code, which is called FLUENT
iv) Designing and improving an MAV design with respect to aerodynamic characteristics

CHAPTER 2

LITERATURE REVIEW

2.1 UNMANNED AERIAL VEHICLES (UAV)

Goraj Z. [6] stated a few UAV problems due to especially ineffective aerodynamic control. One of them is about DarkStar AV#1 crashed in May 1998 on its second flight due to interactions between the landing gear and the vehicles inertia which caused an undamped oscillation and it is not predicted by the system simulation available at that time. The failure of DarkStar is due to ineffective aerodynamic controls during the takeoff roll.

The data shows that not only control system is important for maintaining a UAV on air but also the importance of aerodynamic characteristic.

Research has been done from all over the world on UAV, namely UAV control system, UAV aerodynamic characteristic by using computational and experimental method.

In National University of Singapore, a complete structural Unmanned Flying Wing Air Vehicle is constructed by using ultra light weight composite Kevlar fibre and aerodynamic data of a pre-existent Unmanned Flying Wing Air Vehicle is generated. It uses reverse engineering to analyze and synthesize the model. The techniques used are 3D laser profile scanning of reflex airfoil and fuselage, material research and selection, weight and balance matching techniques and CFD program which is called FLUENT to generate aero coefficients and forces to estimate aerodynamic centre [7].

In University of Concepcion, Chile, an autonomous operating aircraft is created, by using a small and simple RC aircraft which is called Kadet and installed with commercially available flight control system. The new creation is named GIANT 3 (abbreviation of Grupo de Interes Aviones No Tripulados = UAV special interest group). The journal describes methodology used to determine mass and inertia contribution, lifting surface analysis and measurement of dimensions of aircraft to redesign the UAV such as implementation of high lift system, twin engine layout, drag cleanup, robust flight control and optimization of propulsion system. A dynamical model is build based on system matrix that identifies dynamical properties. Analysis tools such as XFOIL, XFLR5 and AVL are used. To validate the model, flight tests such as manoeuvres like inducing eigenmotions like phugoide, dutchroll and spiral are conducted [8].

Landman D.et al [9] had tested on a production model of UAV, which has 3.35m wing, 114kg maximum takeoff mass and a cruise speed of 148 kph, is tested by using Langley Full Scale Tunnel (LFST). The UAV is designed for tactical short range optical/ electronic surveillance, radio relay and training mission. The LFST is the second largest wind tunnel in United States, operates in Old Dominion University, under a Memorandum of Agreement with NASA Langley Research Centre. Force and moment data are found to investigate longitudinal and lateral aerodynamic characteristic, with and without power, for several payload configuration such as BWT, PODB and BALL. Control effectiveness was determined without power and at cruise power at a single angle of attack. A full scale of power on testing is conducted too to measure net thrust for propeller evaluation. However, details of methodology used and results are not shown in this journal.

In Venezuela, an UAV is designed for petroleum exploration. It is called ANCE (Unmanned Aircraft for Ecological Conservation in Spanish acronym). It uses rectangular wing with 0.254 span and 0.052m chord NACA 0015 airfoil. The aerodynamic characteristic of initial design is further improved by making modifications in landing gear and wing tips. The methods used include numerical method where airfoil analysis computational code VisualFoil is used, and experimental testing by using Wind

Tunnel testing. Polar curves of design were traced. From the modifications made, efficiency is increased by 6% by experimental method and 16% by theoretical method [10].

2.2 MICRO AERIAL VEHICLES (MAV)

In University of Konkuk, a design of precision balance and aerodynamic characteristic measurement system has been done for a micro aerial vehicle (MAV). The author has developed a MAV called Batwing. A precision aerodynamic balance was designed in order to measure lift, drag, rolling moment and pitching moment. The aerodynamic balance was analyzed with finite element method and was calibrated to produce an optimal design. Wind tunnel tests of a 2D airfoil were performed to validate the aerodynamic measurement system [11].

In University of California, Los Angeles, a palmed-sized flapping wing micro aerial vehicle is developed by MEMS Wing technology. It is made of titanium alloy and Paylene-C as wing membrane material. The new MEMS technology enables production of light but robust 3 Dimensional wings, optimized to utilize the flow separation to achieve high lift coefficient. It is equipped with super capacitor-powered and battery powered transmissions system, with flight durations range from 5 to 18 seconds [12].

2.3 NUMERICAL ANALYSIS

In University of Missouri, Columbia, Nathan Logsdon [13] used Gambit and Fluent for numerical analysis for airfoil 0012, where discretized Navier-Stokes equations were solved. The entity boundary condition of edges and pressure far field is selected for 2D and 3D model respectively. Convergence Criteria used is 1E -6. He found out that 2D and 3D model had produced the same results, meaning 2D model can be used to analyze airflow over airfoil instead of time consuming 3D model. He also found out that accurate result can be obtained for angle of attack less than 10 degree.

In University of Concepcion, Andres et al [14] had used CFD code, which is called FLUENT to simulate flow around a low speed acrobatic plane, ENAER T-35 Pillian (which is used for military training). Modeling had been done in three stages, which are modeling of airfoil, 3D wing without fuselage and simplified configuration of the airplane. The Pressure far-field boundary condition is used for the domain and wall for the airplane skin. Several turbulence models had been chosen, for example k-E model (Standard, Realizable, RNG) and S-A (Spalart- Allmaras). The lift curve comparison and pressure coefficient distribution for the measured NACA and CFD results were plotted.

Mueller T.J. et al [15] showed CFD experiment result of aerodynamic characteristic on different wing models including Rectangular, Zimmerman, Inverse Zimmerman and Elliptical with varying of Angles of Attack, Aspect Ratio and Reynolds number. Figure 2.1 shows graph of Lift Coefficient, C_L versus Angles of Attack, α of Aspect ratio 1 and Reynolds number 10^5 for Rectangular, Zimmerman and Inverse Zimmerman wingspan. As Angle of Attack increases, Lift Coefficient increases, until a maximum angle and Lift Coefficient decreases.

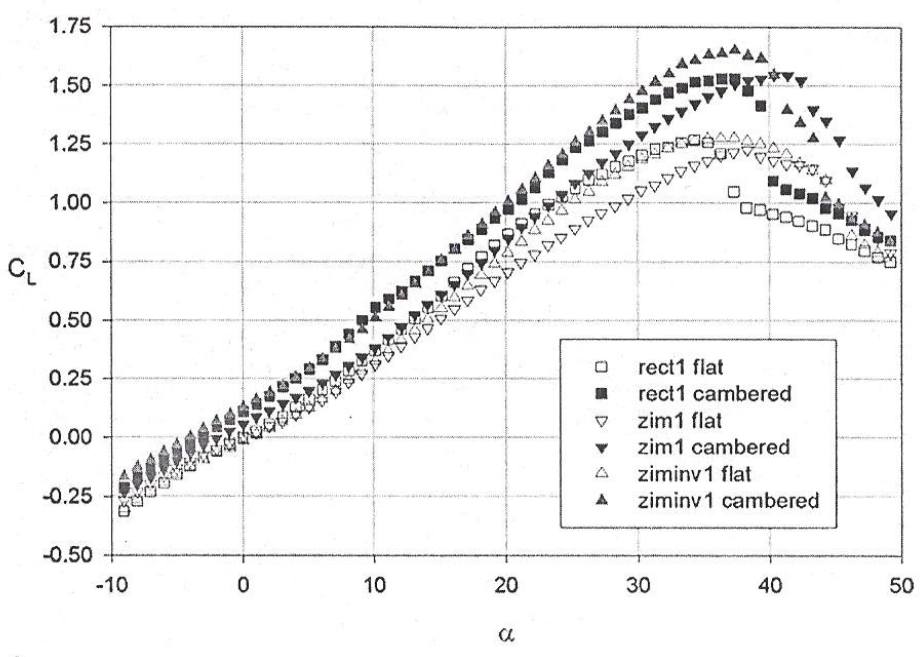

FIGURE 2.1: C_L (Lift Coefficient) versus α (Angles of Attack), AR= 1.00, Re = 10^5 [15]

Figure 2.2 shows graph of Lift Coefficient, C_L versus Angles of Attack, α of rectangular plan form, with varying of aspect ratio. Aspect ratio is one of the important parameter affecting the aerodynamic characteristic. Lower aspect ratio shows higher Lift Coefficient below 0 deg Angle of Attack. Above 0 deg Angle of Attack, higher aspect ratio shows higher Lift Coefficient. Above certain angle, lower aspect ratio shows higher Lift Coefficient. Other observations include for an aspect ratio above 1.25, most plan forms exhibit lift curves that are more linear [15].

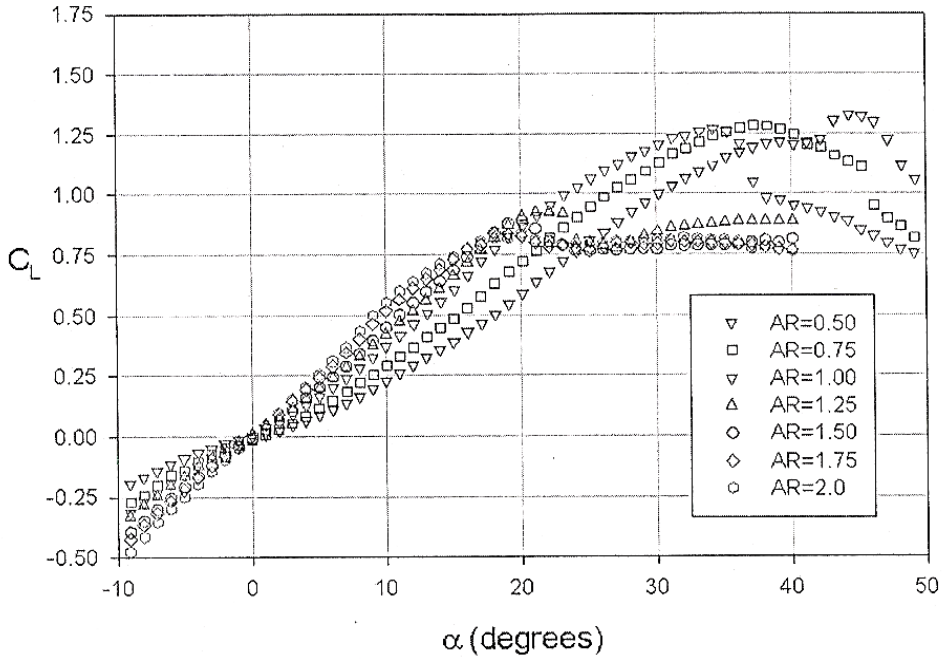

FIGURE 2.2: C_L (Lift Coefficient) versus α (Angles of Attack), AR= 1.00, Re = 10^5 [15]

Kellogg J.C. et al [15] showed CFD experiment result of aerodynamic coefficient of an MAV named MITE. MITE 1 has 15cm wingspan. MITE 2 is improved to 36.8cm. The CFD code used is Finite Element Flow solver (FEFLO). Figure 2.3 and Figure 2.4 show aerodynamic coefficient for MITE 2. As Angle of Attack increases, Lift Coefficient increases.

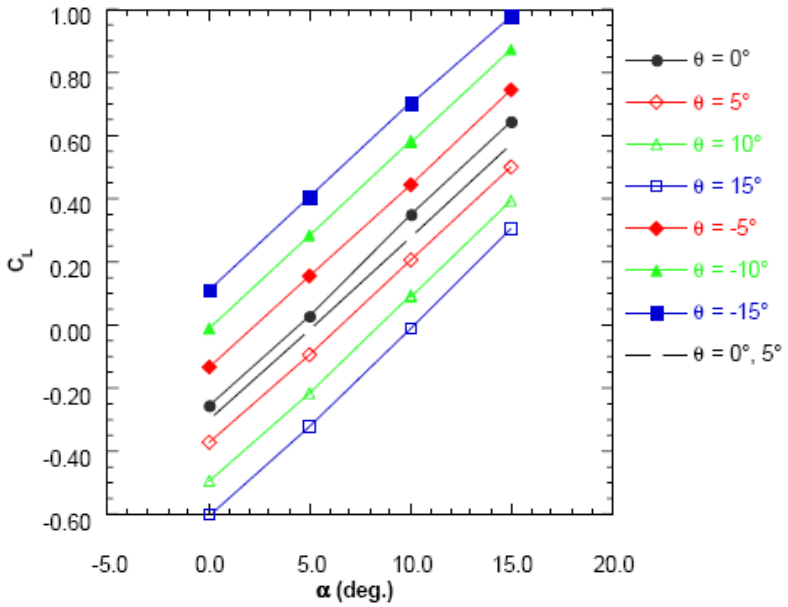

FIGURE 2.3: C_L (Lift Coefficient) versus α (Angles of Attack) for MITE 2 [15]

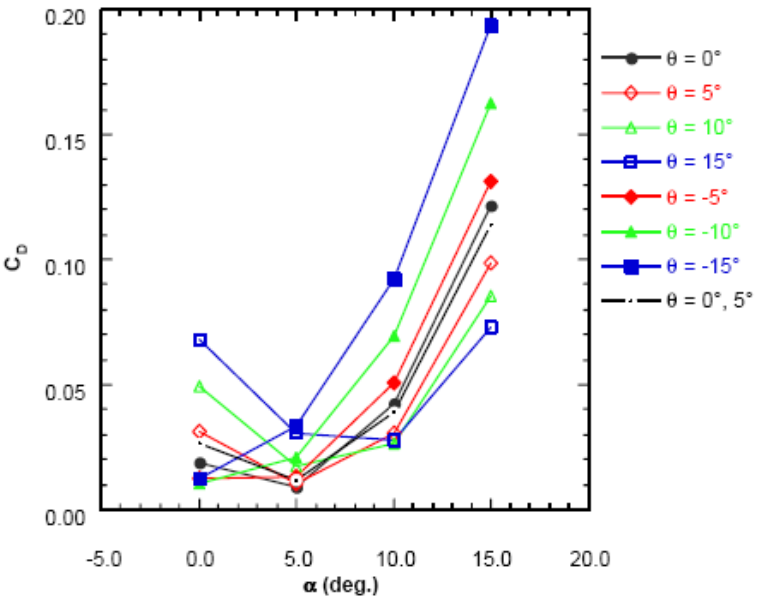

FIGURE 2.4: C_D (Drag Coefficient) versus α (Angles of Attack) for MITE 2 [15]

IFJU P.G. et al [15] had shown CFD experiment result of aerodynamic coefficient of two types of flexible wing MAVs which are batten reinforced and perimeter reinforced wing with rigid wing MAV as reference. Figure 2.5 shows graph of C_L (Lift Coefficient) versus α (Angles of Attack) for rigid, batten reinforced and perimeter reinforced wing at velocity of 13 m/s. As Angle of Attack increases, Lift Coefficient increases. The graph shows stall angle at Angle of Attack of 20 deg.

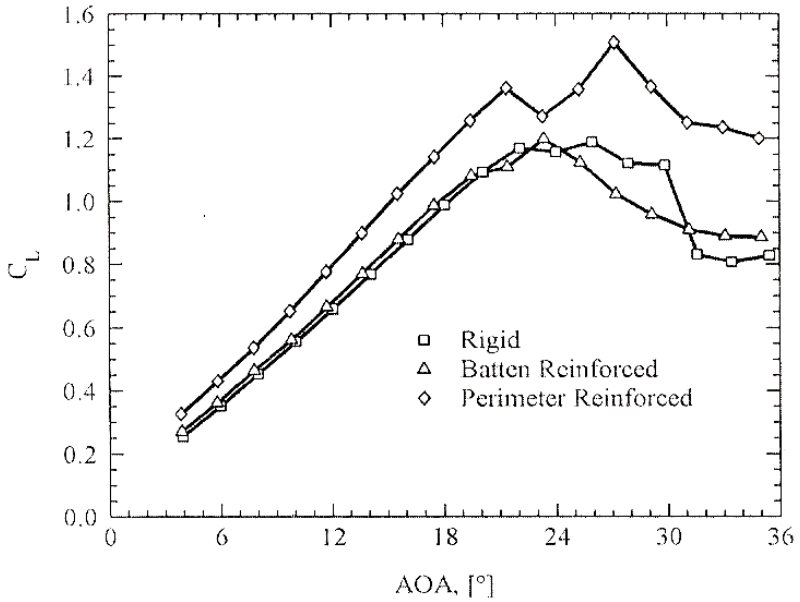

FIGURE 2.5: C_L (Lift Coefficient) versus α (Angles of Attack) for rigid and flexible wings at velocity of 13 m/s [15]

CHAPTER 3

METHODOLOGY

The methodology used in this project includes research for better understanding (Literature Review), Preliminary Design and Numerical testing (CFD simulation). It is summarized in Figure 3.1.

FIGURE 3.1: Methodology Flow Chart

The following sections discuss on research, preliminary design and numerical testing.

3.1 RESEARCH (LITERATURE REVIEW)

Literature review includes research on history of UAV, importance of aerodynamic characteristic of UAV and research done on improving aerodynamic characteristic of an UAV and MAV by using computational or experimental method.

3.2 PRELIMINARY DESIGN

After literature review, a simple design of an UAV is sketched as draft.

3.3 NUMERICAL TESTING (COMPUTATIONAL FLUID DYNAMIC –CFD SIMULATION)

Then the preliminary design will be justified by using Computational Fluid Dynamic (CFD) software, FLUENT. It is used for simulation, visualization, and analysis of fluid flow, heat and mass transfer, and chemical reactions and in this project, for modeling flow conditions in and around moving objects. In order to draw shapes and configurations of design, a geometric modeling and grid generation tool, GAMBIT is used, to allow creation of geometry or importing geometry from most Computational Aided Design (CAD) packages. Improvements on MAV design will be made where applicable. After the creation of geometry, it is meshed and exported as mesh file to FLUENT. Two types of meshing method are used. The first type is uniform meshing in a single domain. The second type of meshing method has finer mesh at the region near airplane. The following figures show second meshing method where different meshing sizes are generated in a single domain.

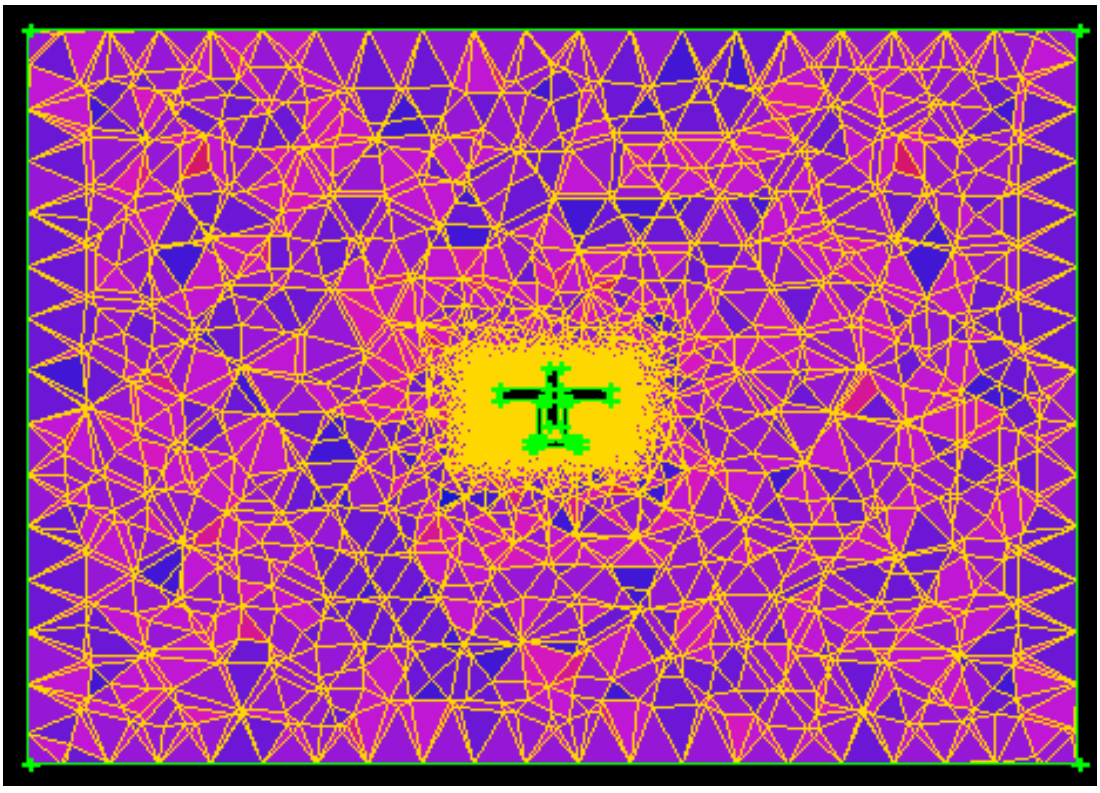

FIGURE 3.2: Top View of Mesh Generated in Airplane Domain

Figure 3.2 shows the top view of mesh generated in the domain. The region near airplane body (yellow region) has finer mesh, and the mesh further from the airplane body is enlarged. This is done to ensure more accurate result in the important region, and reduce computational time at the same time.

Figure 3.4 and Figure 3.6 show mesh generated in the airplane domain in side and front view. Figure 3.3, Figure 3.5 and Figure 3.7 show the zoom-in view of the mesh in top, side and front view.

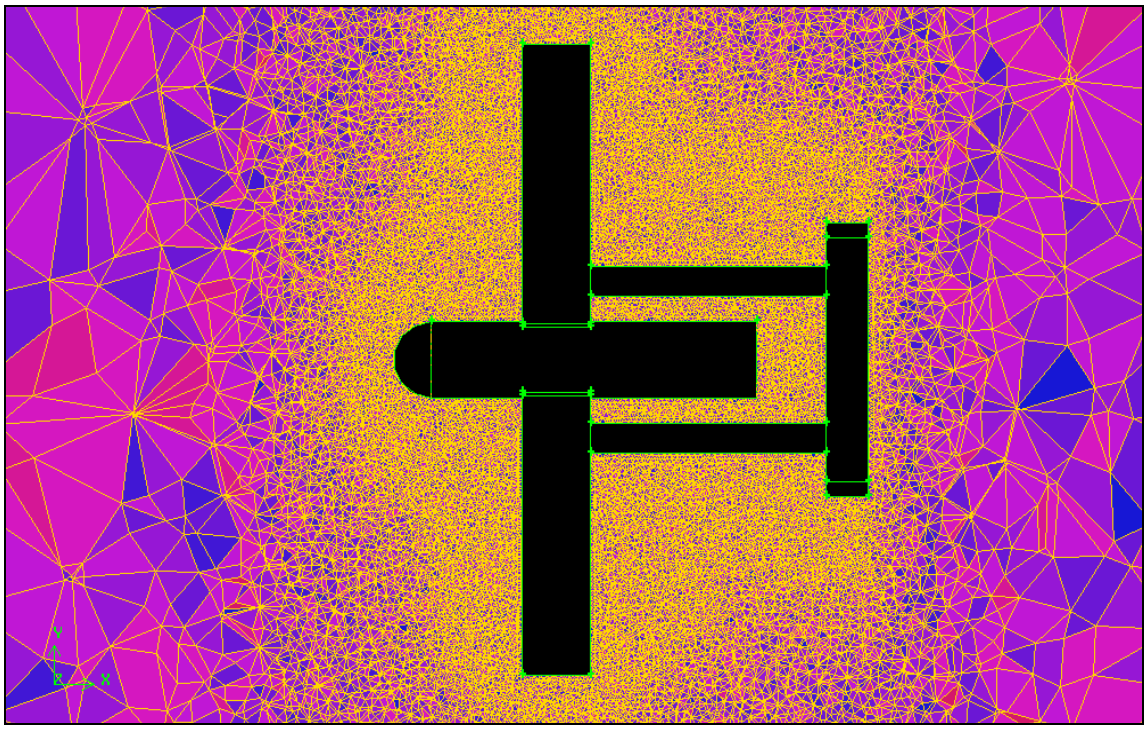

FIGURE 3.3: Zoom-in of Top View of Mesh Generated in Airplane Domain

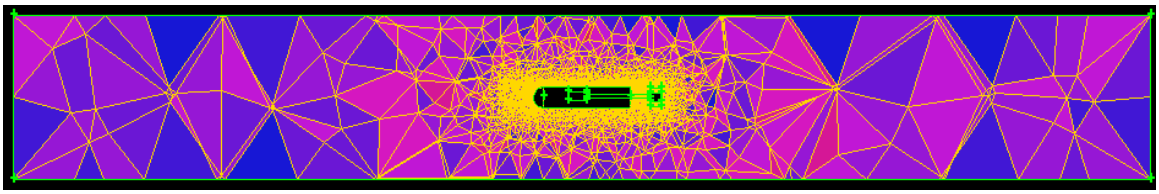

FIGURE 3.4: Side View of Mesh Generated in Airplane Domain

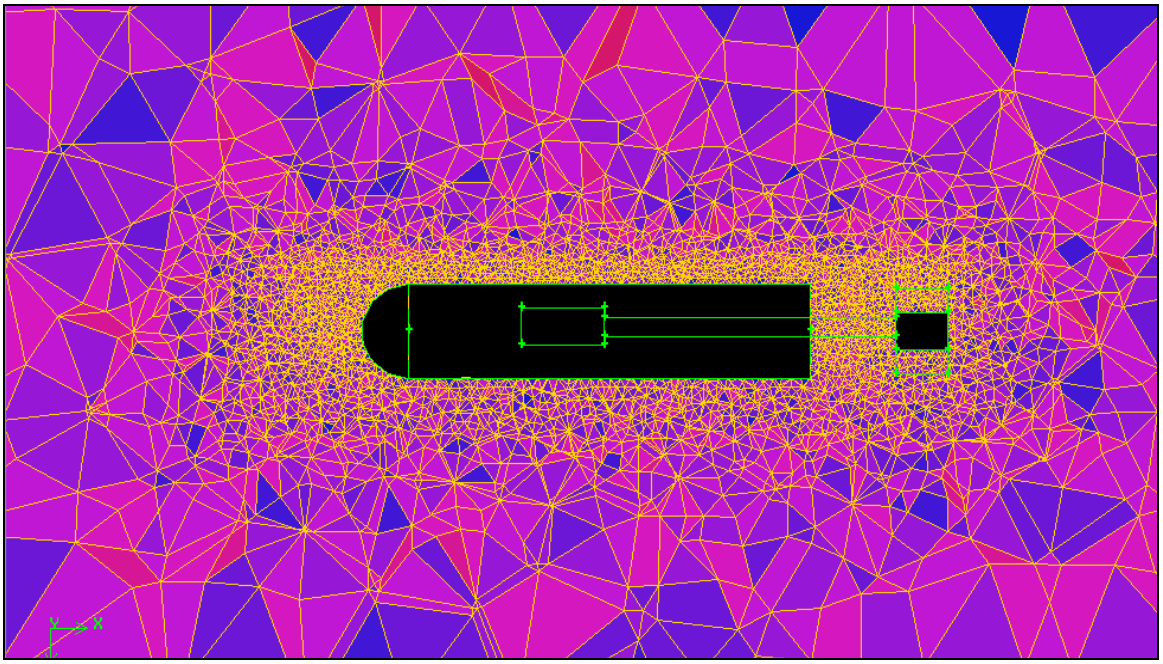

FIGURE 3.5: Zoom-in of Side View of Mesh Generated in Airplane Domain

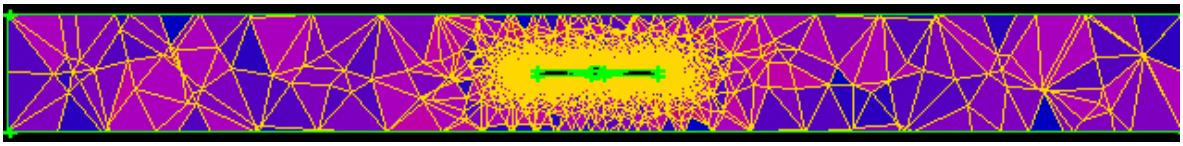

FIGURE 3.6: Front View of Mesh Generated in Airplane Domain

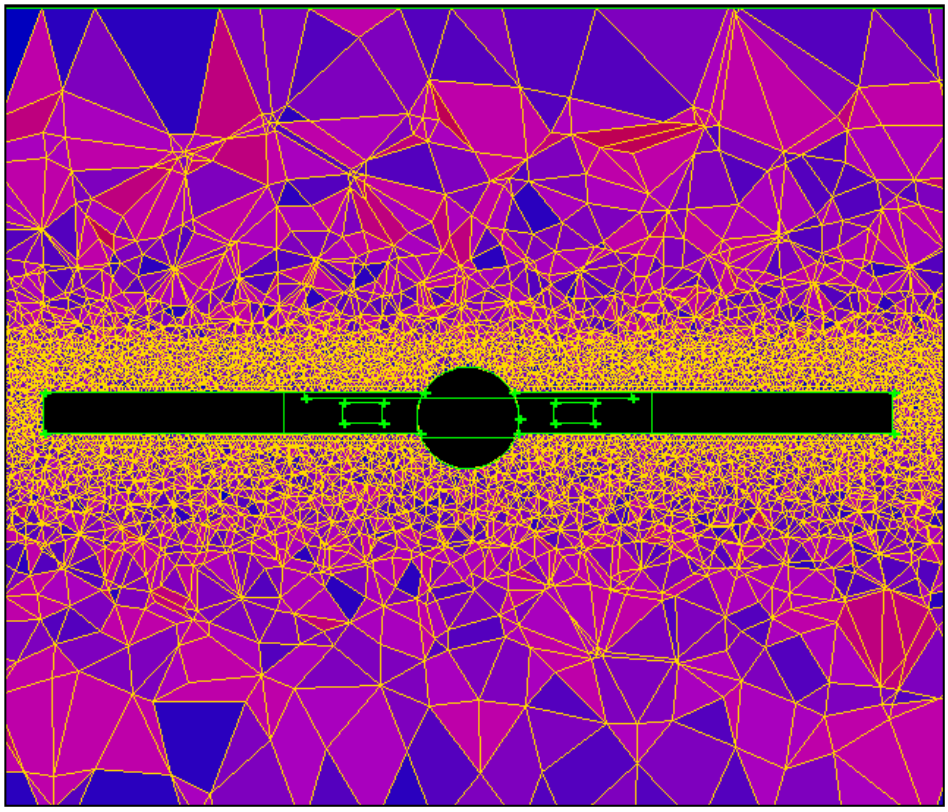

FIGURE 3.7: Zoom-in of Front View of Mesh Generated in Airplane Domain

To set up a numerical problem, a physical model needs to be determined in FLUENT. Then material properties such as fluid, solid or mixture need to be determined too. Next operating conditions, boundary conditions needs to be set before set up solver controls and set up convergence monitors. Then the model will be simulated until the solutions are converged. Figure 3.8 shows the graph of convergence of lift coefficient and Figure 3.9 shows the graph of convergence of drag coefficient.

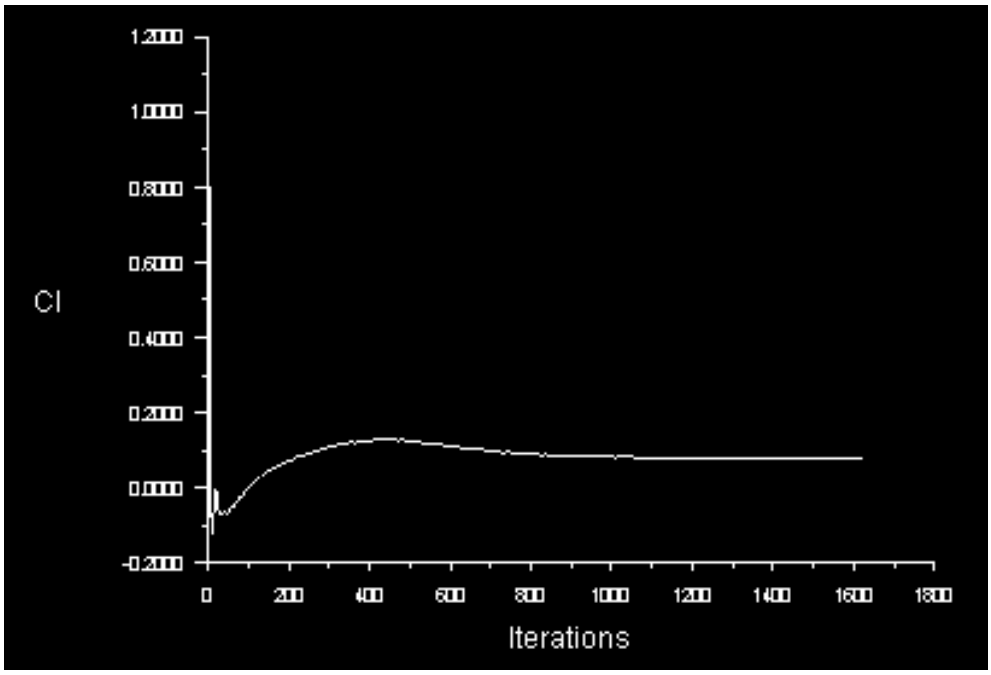

FIGURE 3.8: Graph of Convergence of Lift Coefficient in Fluent Simulation

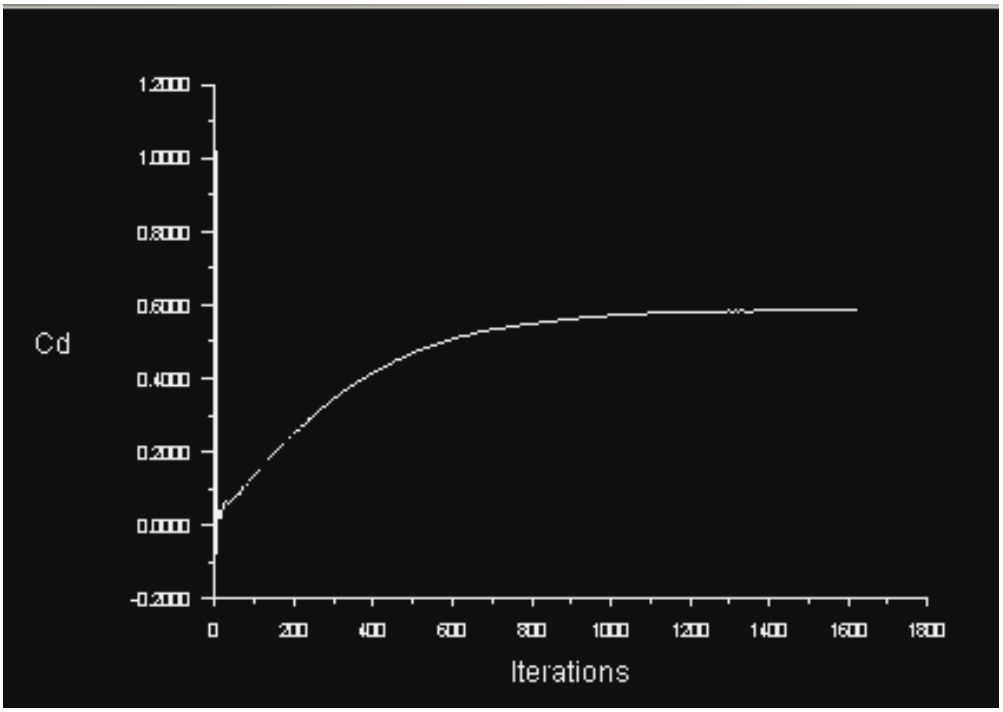

FIGURE 3.9: Graph of Convergence of Drag Coefficient in Fluent Simulation

CHAPTER 4

RESULTS AND DISCUSSIONS

4.1 MAV DESIGN 1

A simple and basic shape of MAV has been draft and started to be modelled by using GAMBIT, the geometric modelling and grid generation tools. The basic type of MAV is chosen based on the simplicity of shape and it is a common type of UAV geometry used. This airplane consists of a rectangular body, rectangular wing, tail and supports of the wing which connect between wing and tail. Operation command of GAMBIT have been learnt in order to model the preliminary design. The first draft of the design is showed in Figure 4.1. This simple rectangular body shape airplane is named Design 1.

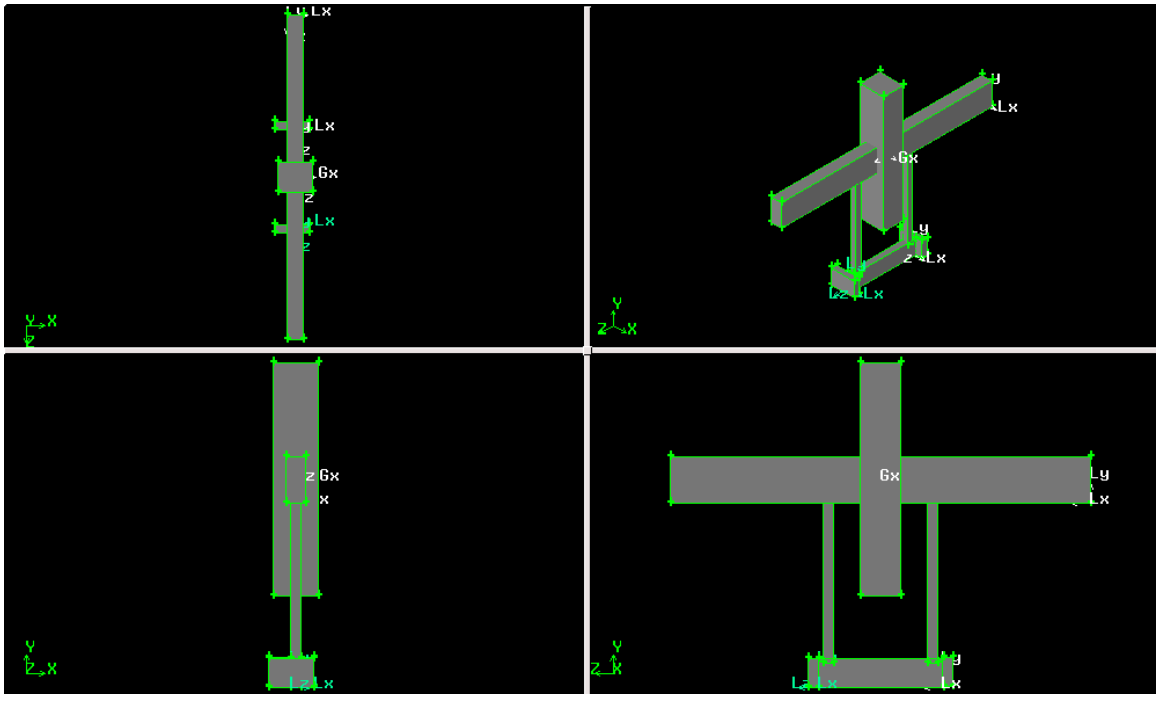

FIGURE 4.1: Four Views of MAV preliminary design by using GAMBIT (Design 1)

In GAMBIT, meshing and defining of boundary conditions are done before exporting as mesh file to FLUENT. The first simulation is done by the following assumption: viscous model as K-ε model, face boundary conditions as wall of computer domain as wall and the face parallel to airplane front face as velocity inlet, velocity of velocity inlet as 40 m/s. The airplane boundary condition is set to wall. The boundary condition for computer domain is set as velocity inlet and the face parallel to the back of the airplane as pressure outlet. The solutions of this simulation converged. The result shows that the value for lift coefficient is -0.098. The negative value of lift coefficient is not desired. The velocity and static pressure contour are shown in Figure 4.2 and Figure 4.3.

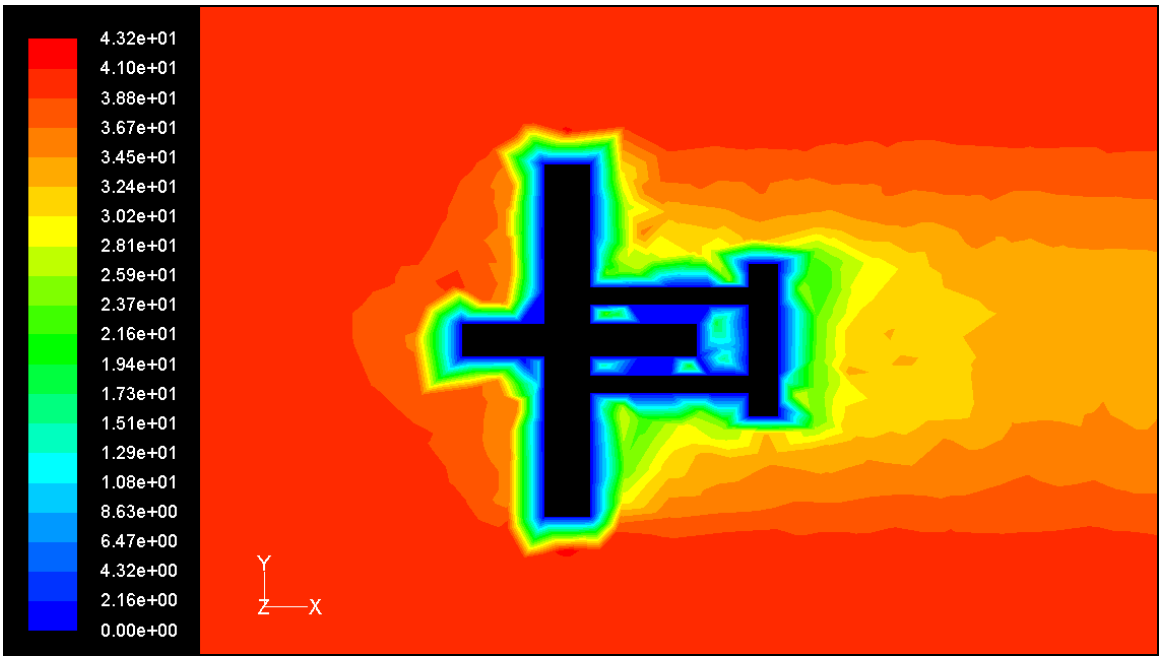

FIGURE 4.2: Velocity contours of MAV Design 1 (Case 1)

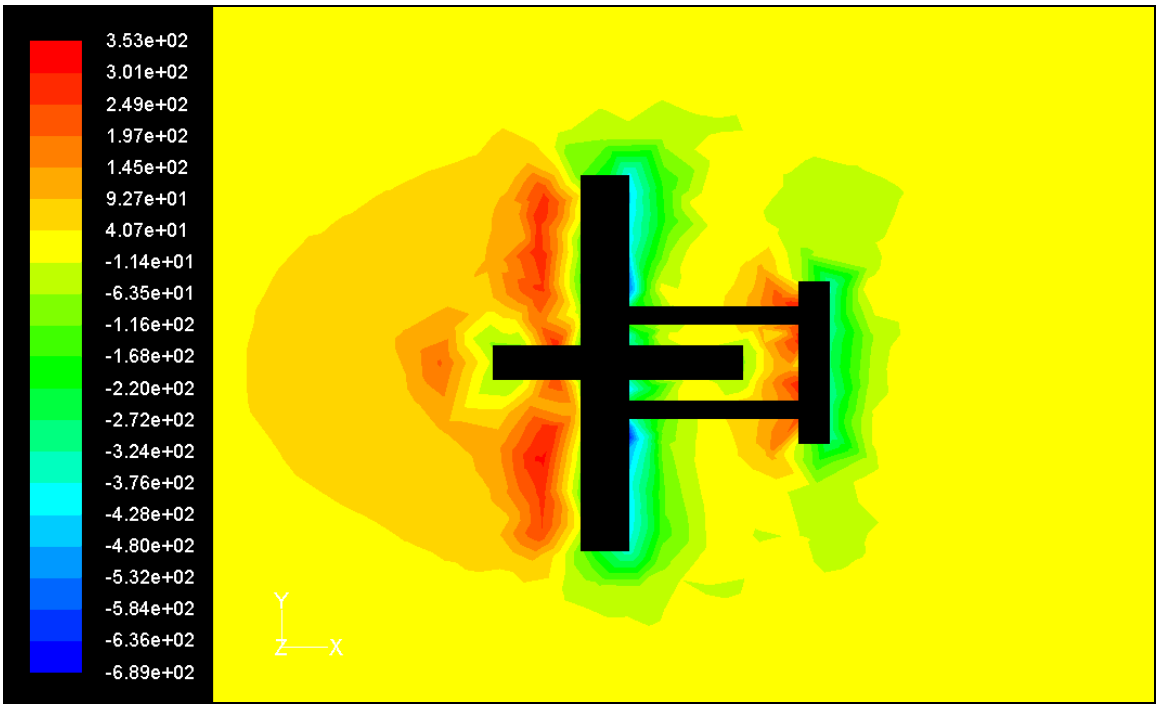

FIGURE 4.3: Pressure contours of MAV Design 1 (Case 1)

The assumptions for simulation are then modified. For case 2, the boundary conditions for other wall of computer domain are set as pressure far- field and only the face parallel to the front face of airplane is set as velocity inlet. The boundary condition for airplane faces is remained as wall. The residual value is increased from 1E-6 to 1E-2 in order to get converged solution. The lift coefficient showed from the result is 0.00279 and drag coefficient 67.361. The lift coefficient is reasonable, but the drag coefficient is not reasonable as compared to the published result. The velocity and pressure contour are shown in Figure 4.6 and Figure 4.8 and for better view in zoom-in Figure 4.7 and Figure 4.9.

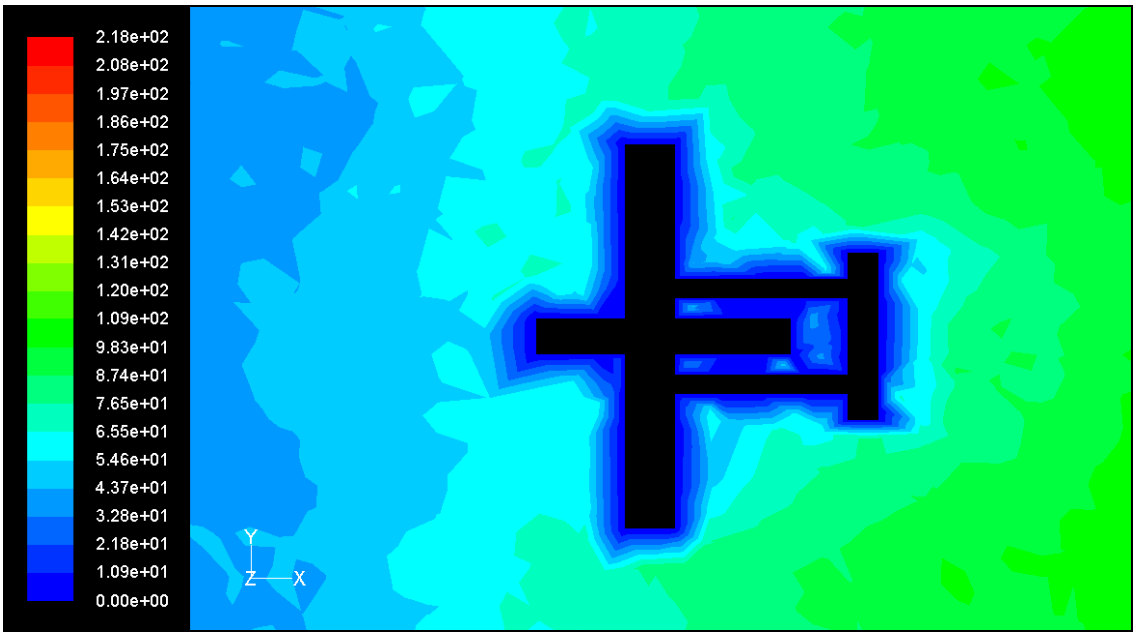

FIGURE 4.4: Velocity contours of MAV Design 1 (Case 2)

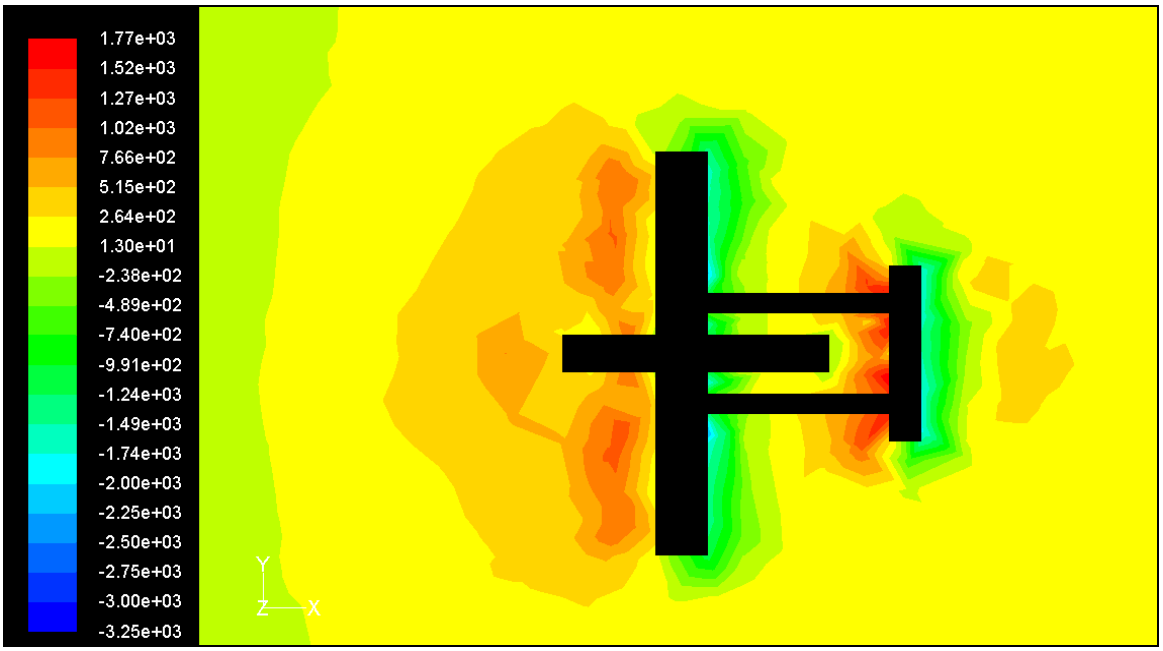

FIGURE 4.5: Pressure Contours of MAV Design 1 (Case 2)

4.2 MAV Design 2

For comparison, the rectangular body is improved to curved shape with the same dimension. It is shown in Figure 4.6.

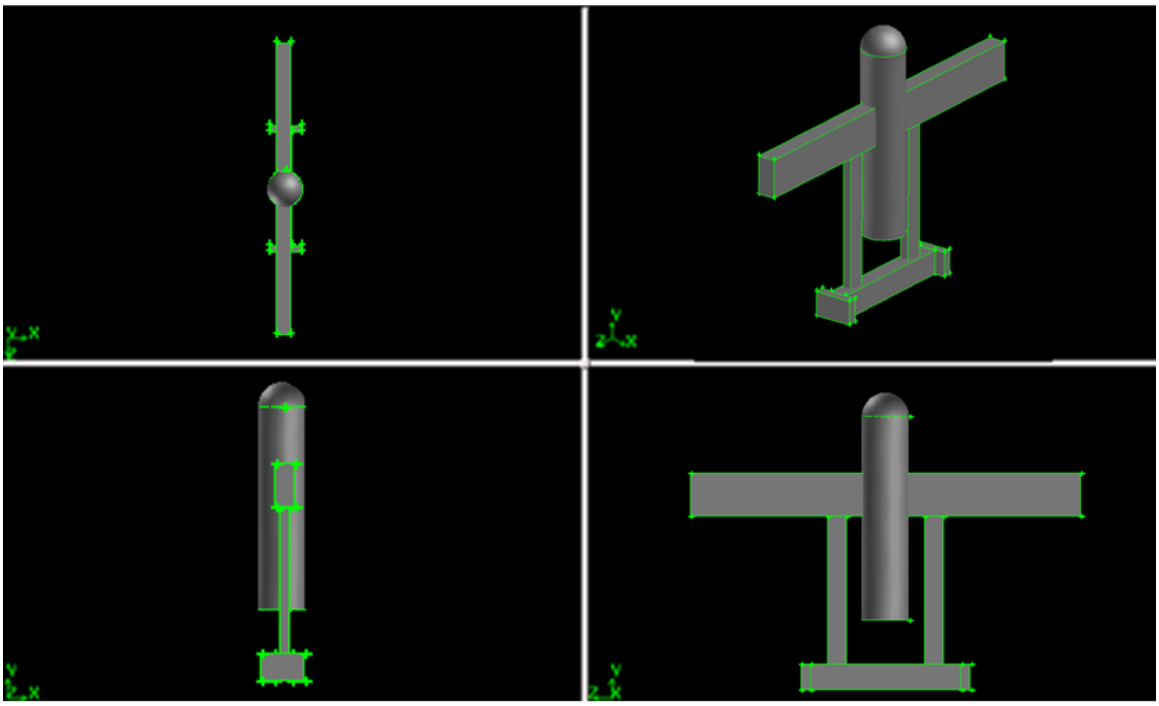

FIGURE 4.6: Four Views of MAV (Design 2)

The simulation is then tried again on an improved curved shape of a plane body, with the same setting with the Design 1. The result for this simulation shows that the lift coefficient for the airplane has been increased as compared to Design 1 to 8.2447. The drag coefficient has been decreased to 58.7055. This is reasonable as the front area has been changed to curved shape, the lift coefficient should increase and the drag coefficient should decrease. The velocity and pressure contour are shown in Figure 4.7 and Figure 4.8.

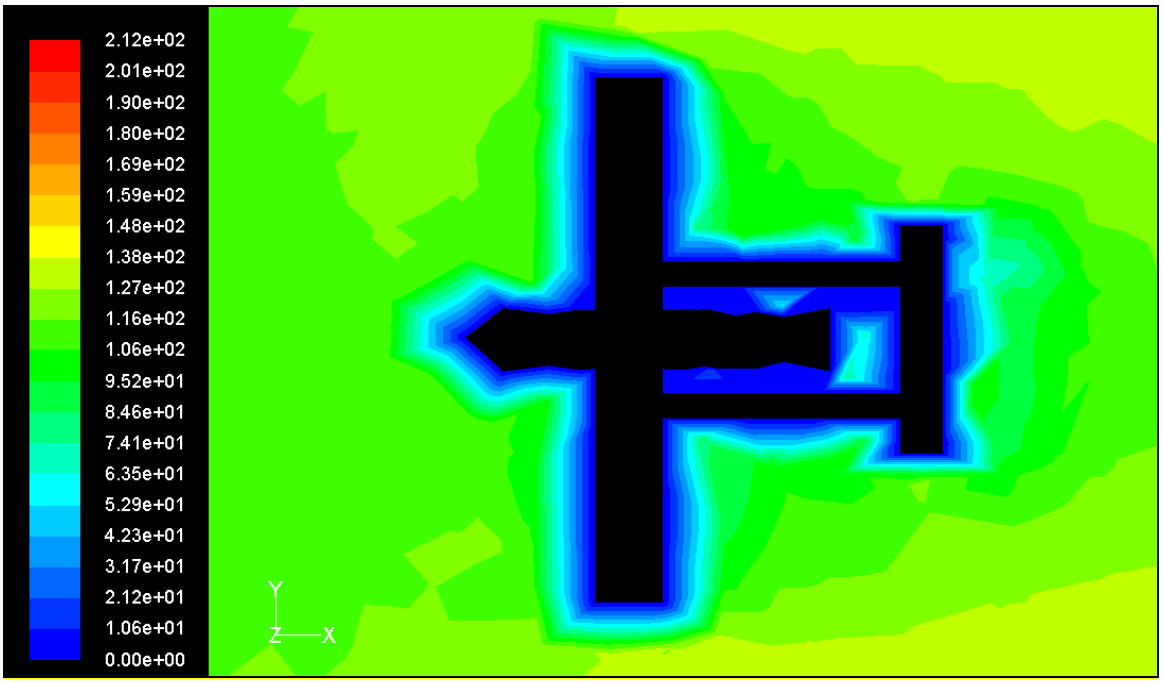

FIGURE 4.7: Velocity Contours of MAV Design 2 (Case 3)

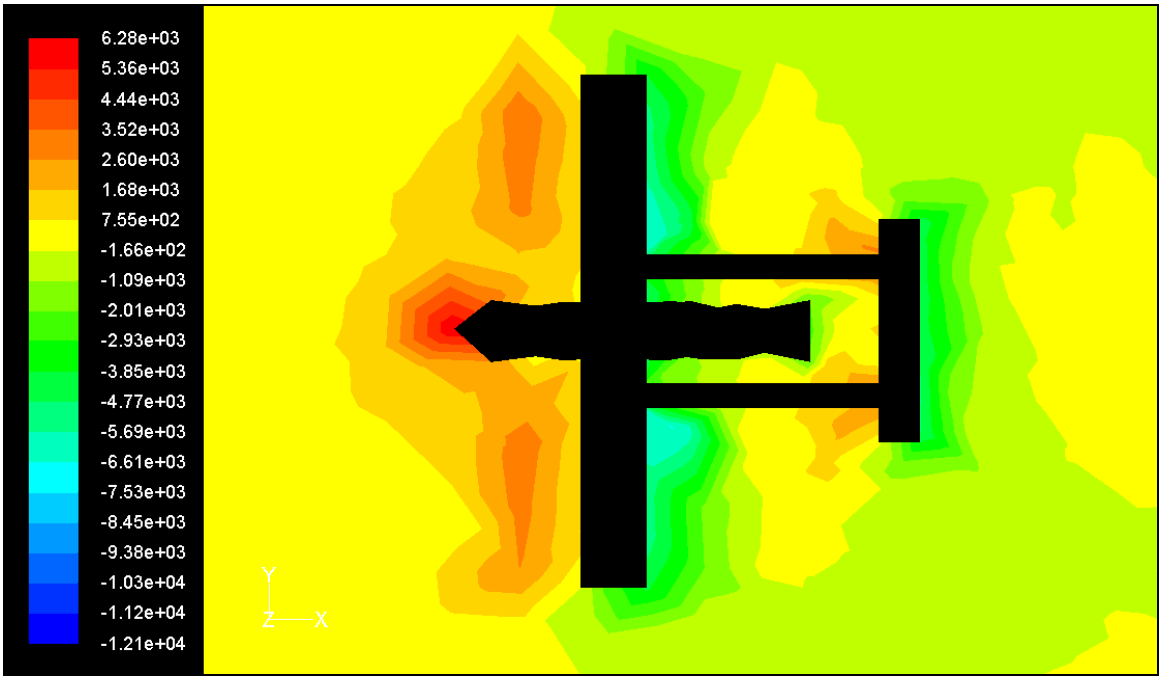

FIGURE 4.8: Pressure Contours of MAV Design 2 (Case3)

In Case 3, the mesh size near the surface of airplane is decreased to increase result accuracy. Case 3 is done to Design 2 only. The finest mesh size used is 0.002m while the coarsest mesh size used is 0.02m. Thus, the number of mesh size is increased. The result is shown in Table 4.1. The velocity and pressure contours are shown in Figure 4.9 and Figure 4.10.

TABLE 4.1: Result of Lift and Drag Coefficient for 0 deg AOA

Airplane Design	Lift Coefficient	Drag Coefficient
Design 1	-0.00102	0.0279
Design 2	0.00238	0.0158

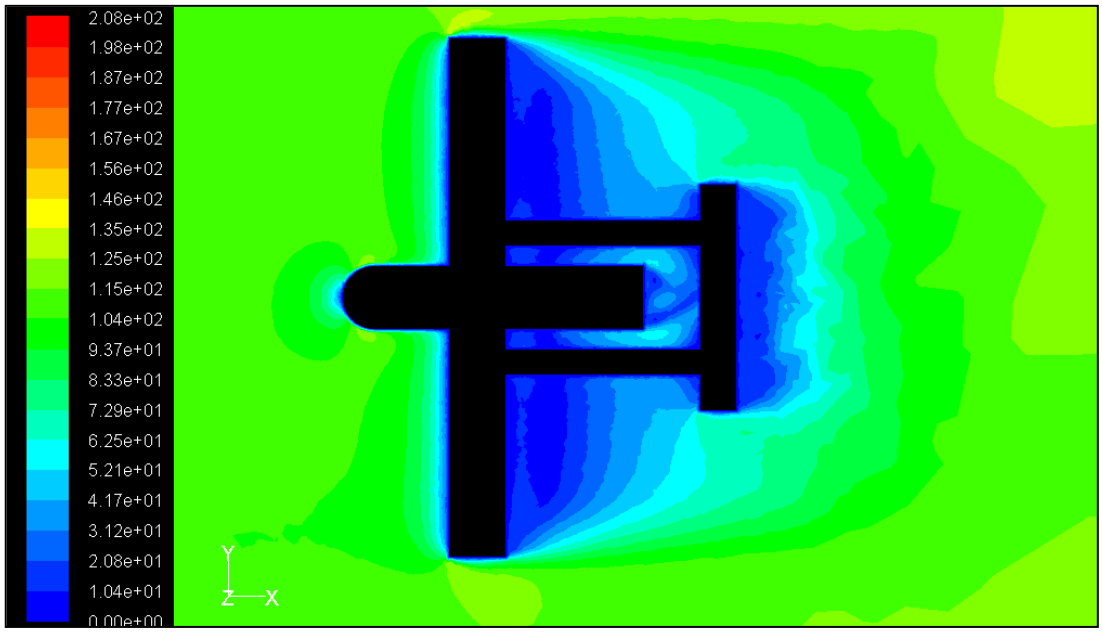

FIGURE 4.9: Velocity Contours of MAV Design 2, Finer Meshing (Case 3, V=40 m/s)

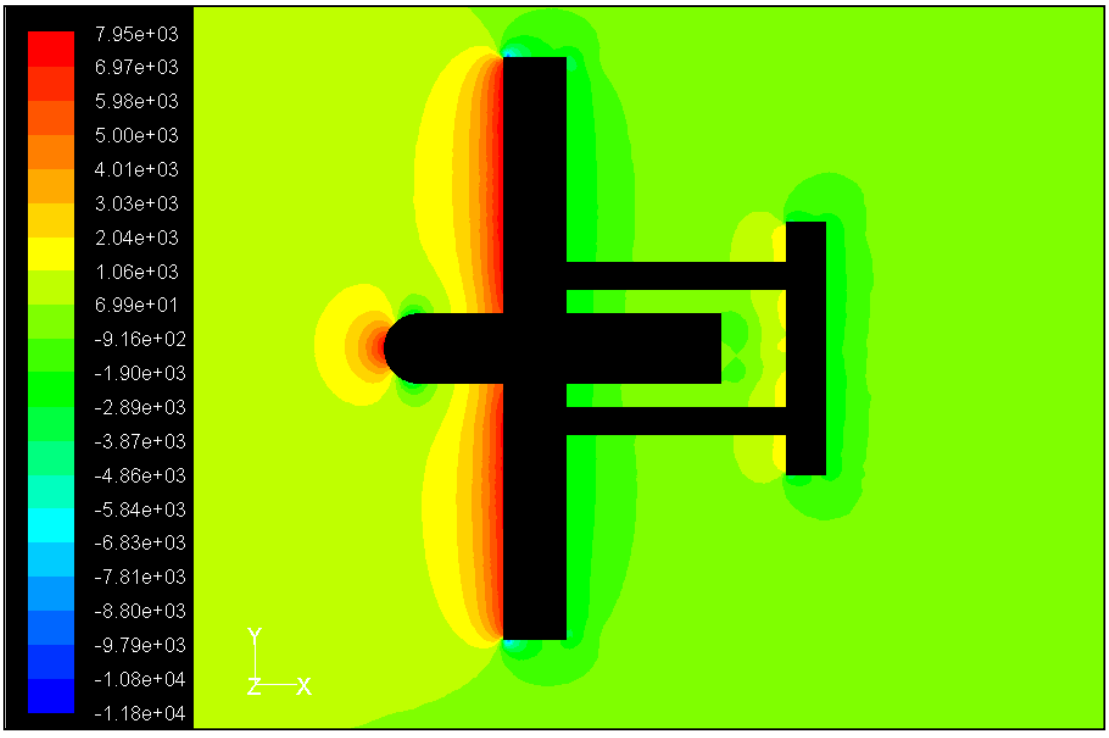

FIGURE 4.10: Pressure Contours of MAV Design 2, Finer Meshing (Case 3, V= 40 m/s)

From paper published, it is suggested that range of an MAV speed is from 24 to 63km/h, which means 6 to 17 m/s. Hence the velocity is changed from 40m/s to 10m/s and simulation is run again. The result is shown in Table 4.2.

TABLE 4.2: Result of Lift and Drag Coefficient for 0 deg AOA

Airplane Design	Lift Coefficient	Drag Coefficient
Design 1	-0.000306	0.0259
Design 2	0.076	0.583

Simulations are run for the MAV Design 2 by using finer meshing from 0 deg AOA (Angles of Attack) to 20 deg AOA (Angles of Attack). The graphs of Lift and Drag Coefficient versus AOA (Angles of Attack) are shown in Table 4.3, Figure 4.11 and Figure 4.12. Velocity and pressure contours are shown in Figure 4.13 and Figure 4.14.

The result is compared with a rectangular wing and a fixed wing MAV published data by Mueller T.J et al [15]. For the rectangular wing, from 0 deg AOA (Angles of Attack) to 15 deg AOA (Angles of Attack), C_L ranges from -0.2 to 0.6. For the fixed wing MAV, from 0 deg AOA (Angles of Attack) to 15 deg AOA (Angles of Attack), C_L ranges from -0.2 to 0.7. The result For MAV Design 2, from 0 deg AOA (Angles of Attack) to 15 deg AOA (Angles of Attack), C_L ranges from 0.076 to 0.227. As Angle of Attack increases, C_L increases, which shows the same C_L and Angles of Attack relationship as the published data. The published results show higher lift than MAV Design 2.

TABLE 4.3: Lift Coefficient (C_L) and Drag Coefficient (C_D) at Different Angles of Attack (AOA) for Design 2

AOA	**C_L**	**C_D**
0	0.076000	0.583000
1	0.086399	0.583845
2	0.096000	0.584960
3	0.107005	0.585921
4	0.117262	0.586729
5	0.127478	0.587382
6	0.137656	0.587880
7	0.148143	0.588195
8	0.158229	0.588383
9	0.168270	0.588414
10	0.178270	0.588284
11	0.188217	0.588010
12	0.198110	0.587563
13	0.207959	0.586944
14	0.217650	0.586190
15	0.227463	0.585246
16	0.237133	0.584152
17	0.246738	0.582908
18	0.256263	0.581476
19	0.265717	0.579875
20	0.275006	0.578002

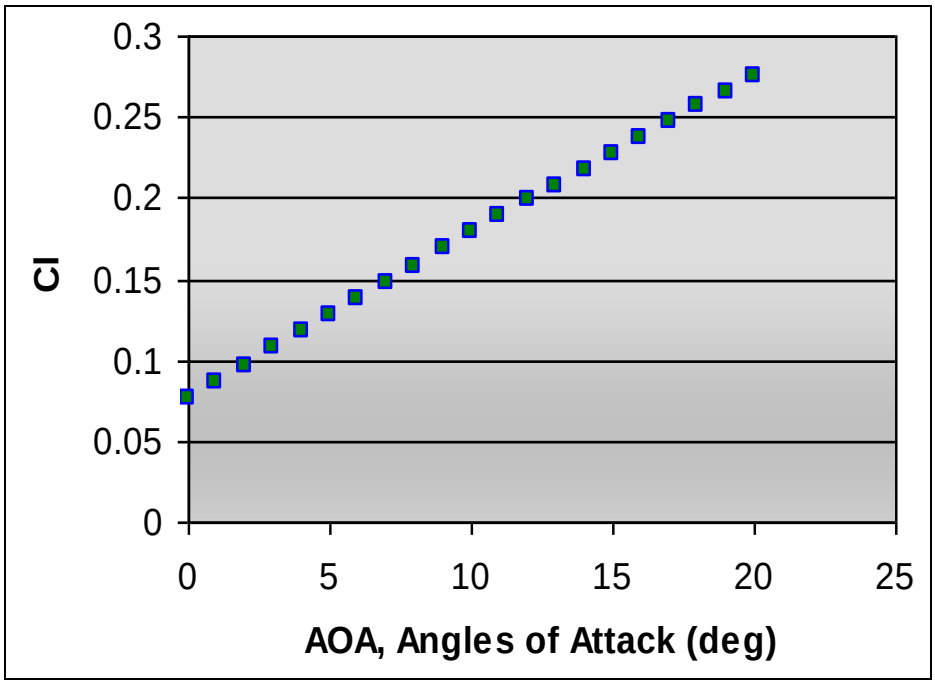

FIGURE 4.11: Lift Coefficient, C_L versus Angles of Attack (AOA) for Design 2

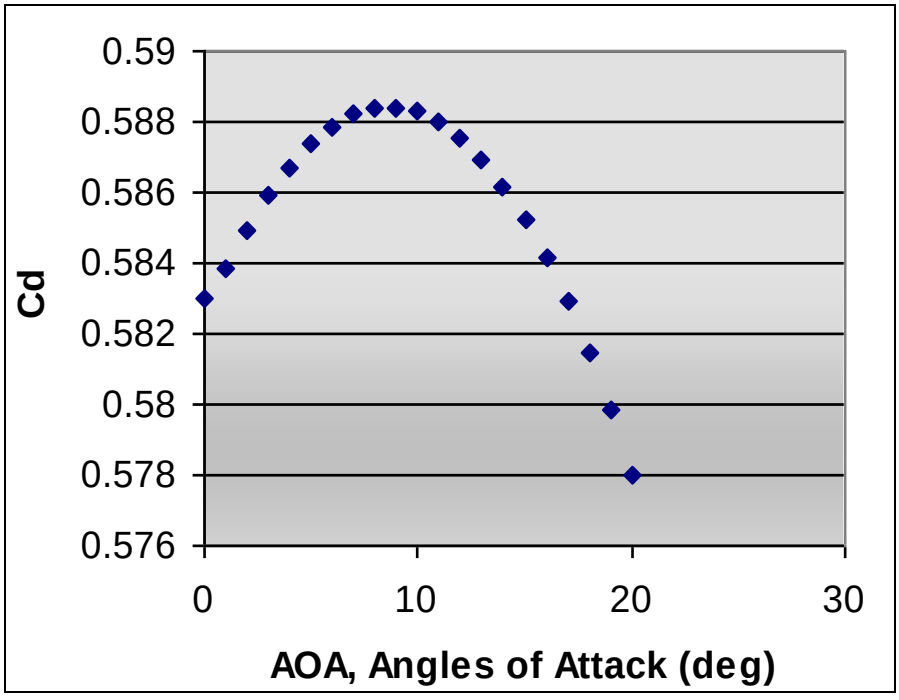

FIGURE 4.12: Drag Coefficient, C_D versus Angles of Attack (AOA) for Design 2

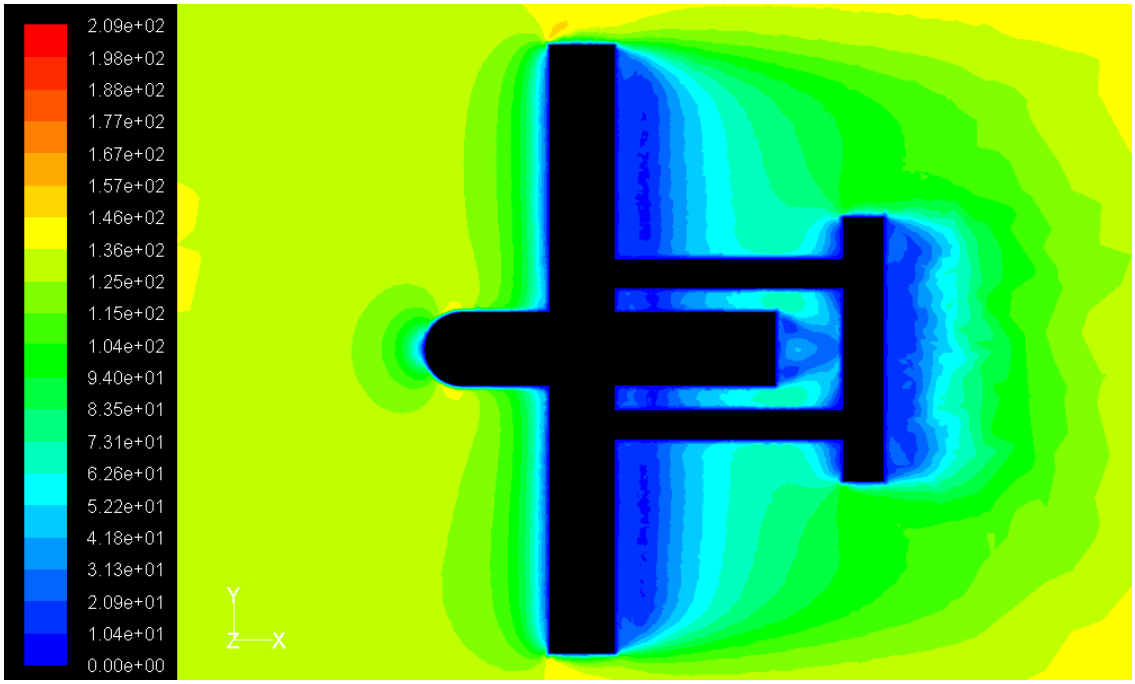

FIGURE 4.13: Velocity Contours of MAV Design 2, Finer Meshing (V= 10 m/s)

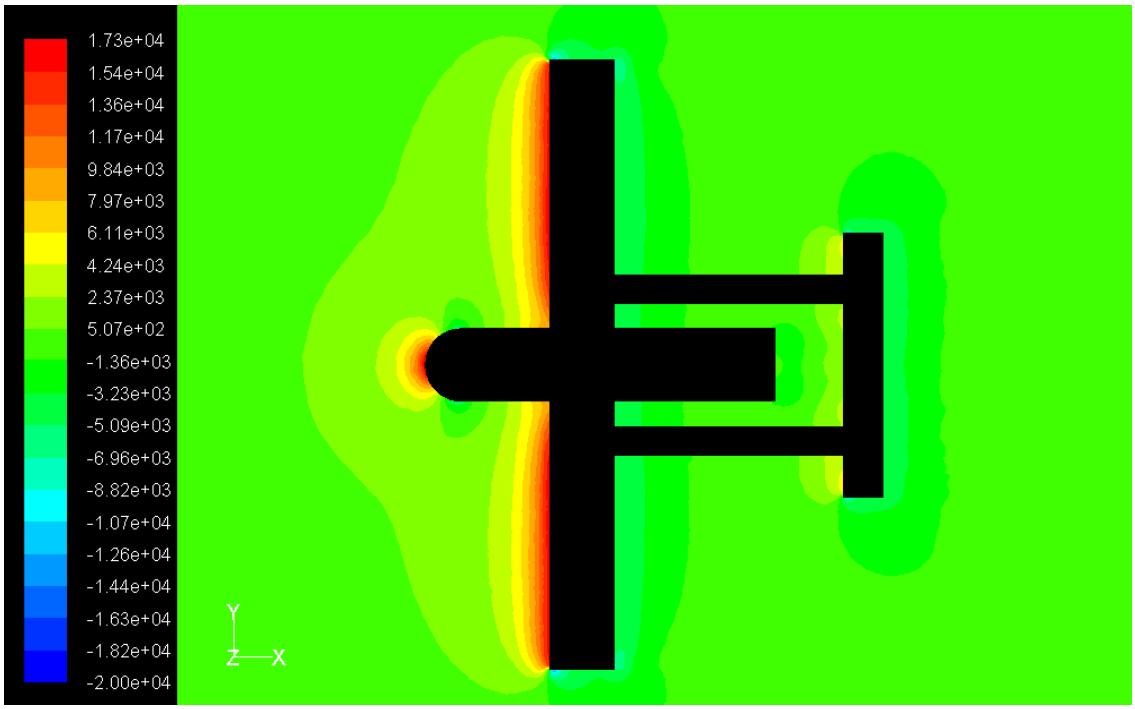

FIGURE 4.14: Pressure Contours of MAV Design 2, Finer Meshing (V= 10m/s)

4.3 MAV Design 3

The curved body profile is further improved. The rectangular wing is improved to front curve shape. The curved front area remains. The shape is shown in the following Figure 4.15. This shape of design is named Design 3.

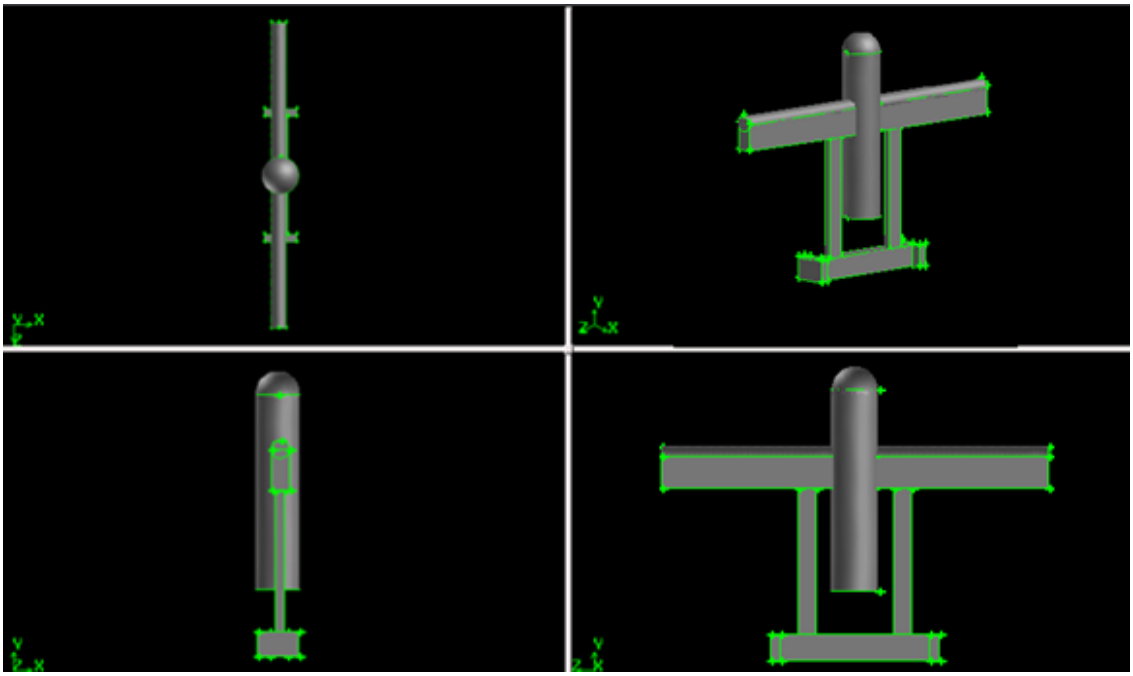

FIGURE 4.15: Four Views of MAV (Design 3)

Simulations are run for the curved body and wing airplane from 0 deg AOA (Angles of Attack) to 14 deg AOA (Angles of Attack), with the same setting of Case 3. The result is shown in Table 4.4, Figure 4.16 and Figure 4.17.

TABLE 4.4: Lift Coefficient (C_L) and Drag Coefficient (C_D) at Different Angles of Attack (AOA) for Design 3

AOA	C_L	C_D
0	-0.01305	0.526024
2	0.006987	0.522249
4	0.024929	0.520941
6	0.043122	0.519028
8	0.061266	0.51651
10	0.079396	0.51342
12	0.097381	0.509687
14	0.11526	0.505357

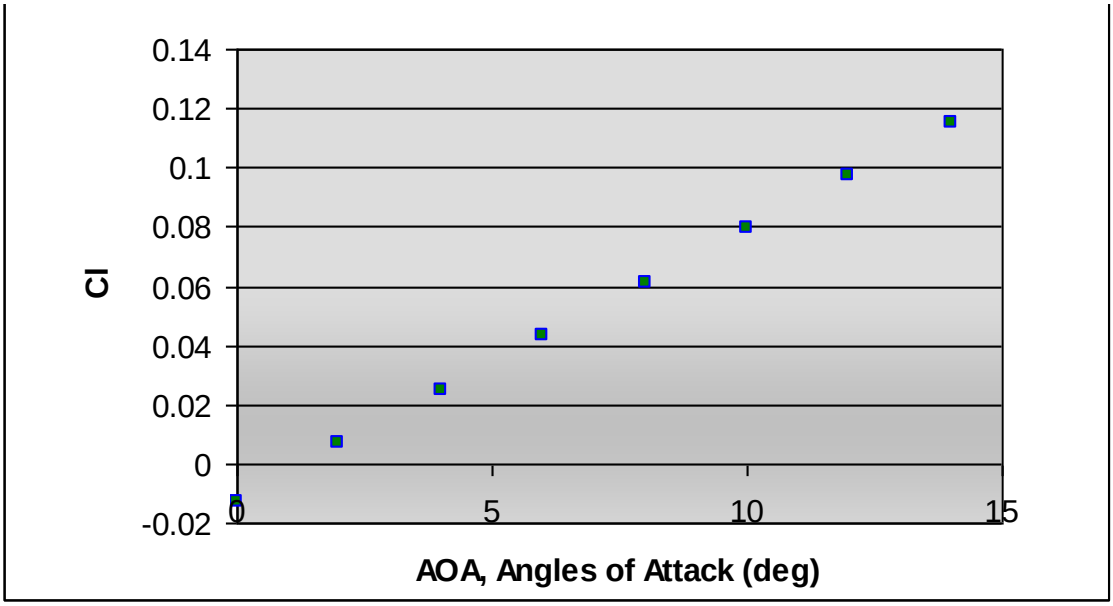

FIGURE 4.16: Lift Coefficient, C_L versus Angles of Attack (AOA) for Design 3

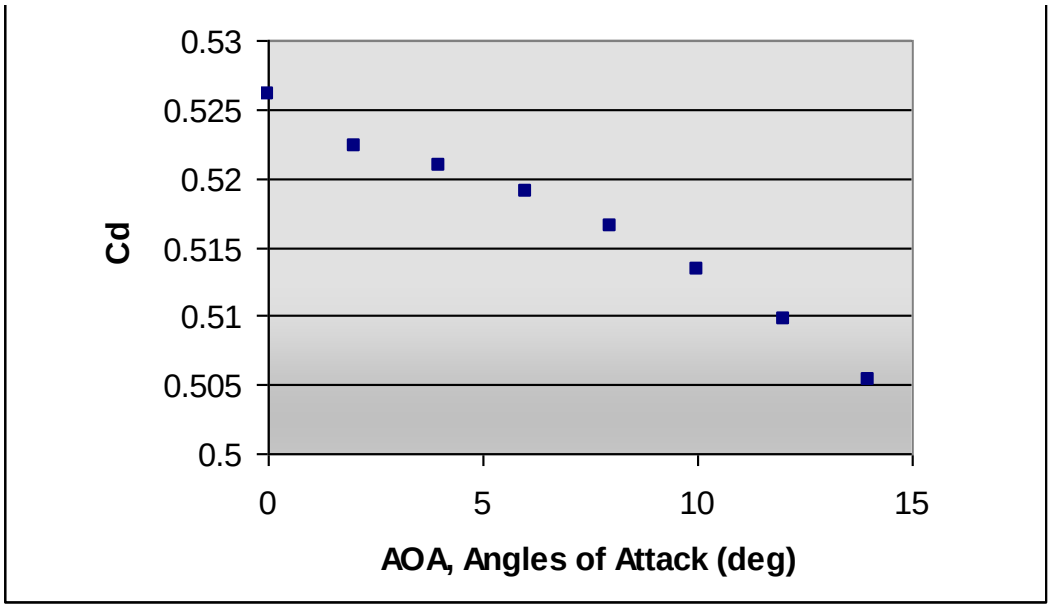

FIGURE 4.17: Drag Coefficient, C_D versus Angles of Attack (AOA) for Design 3

The result of Design 3 is compared with a rectangular wing and a fixed wing MAV published data by Mueller T.J et al [15]. For the rectangular wing, from 0 deg AOA (Angles of Attack) to 15 deg AOA (Angles of Attack), C_L ranges from -0.2 to 0.6. For the fixed wing MAV, from 0 deg AOA (Angles of Attack) to 15 deg AOA (Angles of Attack), C_L ranges from -0.2 to 0.7. The result For MAV Design 3, from 0 deg AOA (Angles of Attack) to 15 deg AOA (Angles of Attack), C_L ranges from -0.01 to 0.11. As Angles of Attack increase, C_L increases, which shows the same C_L and Angles of Attack relation as the published data. The published results show higher lift than MAV Design 3 too. However, result for MAV Design 2 and MAV Design 3 are acceptable.

CHAPTER 5

CONCLUSIONS AND RECOMMENDATIONS

5.1 CONCLUSIONS

Since the first week of confirming of topic chosen, research has been done through journals and reference books in internet and library. Lift is found to be the most important force for flight. Hence numerical testing is done. Preliminary simulation starts on MAV named MAV Design 1. The simulations are continued with improved shape which is named MAV Design 2. The improved design - Curved Shape body- performed much better in higher lift and lower drag as compared with the initial rectangular body design at zero Angles of Attack (AOA). The Curved Shape body airplane is then improved again to Curved body and wing airplane, which is named MAV Design 3. By comparing graph C_L and C_D versus AOA with results published, it shows that the simulations resulted on reasonable predictions of lift and drag coefficients. The calculated results agree with those published for available MAV. The project should be continued by using finer meshing, to achieve more accurate and numerical independent result.

5.2 RECOMMENDATIONS

The project contains of big scopes and should be continued in order to get better results. The computer performance can be improved, hence reducing computational time and the project can be continued to achieve numerically-independent results.

REFERENCES

1. Newcome L.R.N; Unmanned Aviation: A Brief History of Unmanned Aerial Vehicles; *AIAA American Institute of Aeronautics and Astronautics, 2004*.

2. McMichael J.M., Francis M.S.; Micro Air Vehicles – Towards a New Dimension in Flight", *Unmanned Systems, Vol 15, No 3, 1997, pp10-15.*

3. Mueller T.J., Fixed and Flapping Wing Aerodynamics for Micro Air Vehicle Applications, *AIAA, Vol 195, Reston V.A., 2001, p2.*

4. Antonio F.; Flight Performance of Fixed and Rotary Wing Aircraft; *Butterworth-Heinemann, 2006*.

5. Clayton T., Donald F., John A.; Engineering Fluid Mechanics; *Wiley International Edition, 8th edition, 2005.*

6. Goraj.Z ; Dynamic Characteristic of different UAV Configurations ; *Warsaw University of Technology, 11-12 Feb, 2002.*

7. Jayabalan N., Low J.H., Leng G.; Reverse Engineering and Aerodynamic Analysis of a Flying Wing UAV; *Aeronautical Engineering Group of National University of Singapore.*

8. Tinapp F., Elgueta M., Rigot G., Toppinger R.; UAV Aerodynamic Modeling; *University of Concepcion, Chile, 2007.*

9. Landman D, Britcher C, Bennett W.; A Power-on Full-scale Wind Tunnel Test of a UAV; *AIAA American Institute of Aeronautics and Astronautics, 1999.*

10. Pedro J.B, Elsa M.C, Andrea A; Aerodynamic Optimization of an UAV Design; *AIAA American Institute of Aeronautics and Astronautics, 2005.*

11. Suhariyono A., Jong H.K., Nam S.G, Hoon C.P, Kwang J.Y; Design of Precision Balance and Aerodynamic Characteristic Measurement System for Micro Aerial Vehicles; *National Research Laboratory for Active Structures and Materials, Department of Aerospace Engineering, Konkuk University, South Korea, 2006; pp. 92-99.*

12. Nick P.S.T, Tai Y.C, Nassef H, Ho C.M; Titanium Alloy MEMS Wing Technology for a Micro Aerial Vehicle Application; *University of California, Los Angeles, 2001.*

13. Logsdon N, Solbrekken G.; A Procedure for Numerically Analyzing Airfoils and Wing Section; *University of Missouri, Columbia, 2006.*

14. Andres D., Luis E., Rodolfo A.; Aerodynamic Performance Analysis of A Low Speed Acrobatic Airplane by Numerical Simulation ; *University of Concepcion, Chile ; Mecanica Computacional Vol XXI, 2002; pp. 378-391.*

15. Mueller T.J., Kellogg J.C., Ifju P.G, Shkarayev S.V.; Introduction to the Design of Fixed-Wing Micro Air Vehicles Including Three Case Studies; *AIAA American Institute of Aeronautics and Astronautics, 2007.*

APPENDICES

APPENDIX I
MAV DESIGN 1

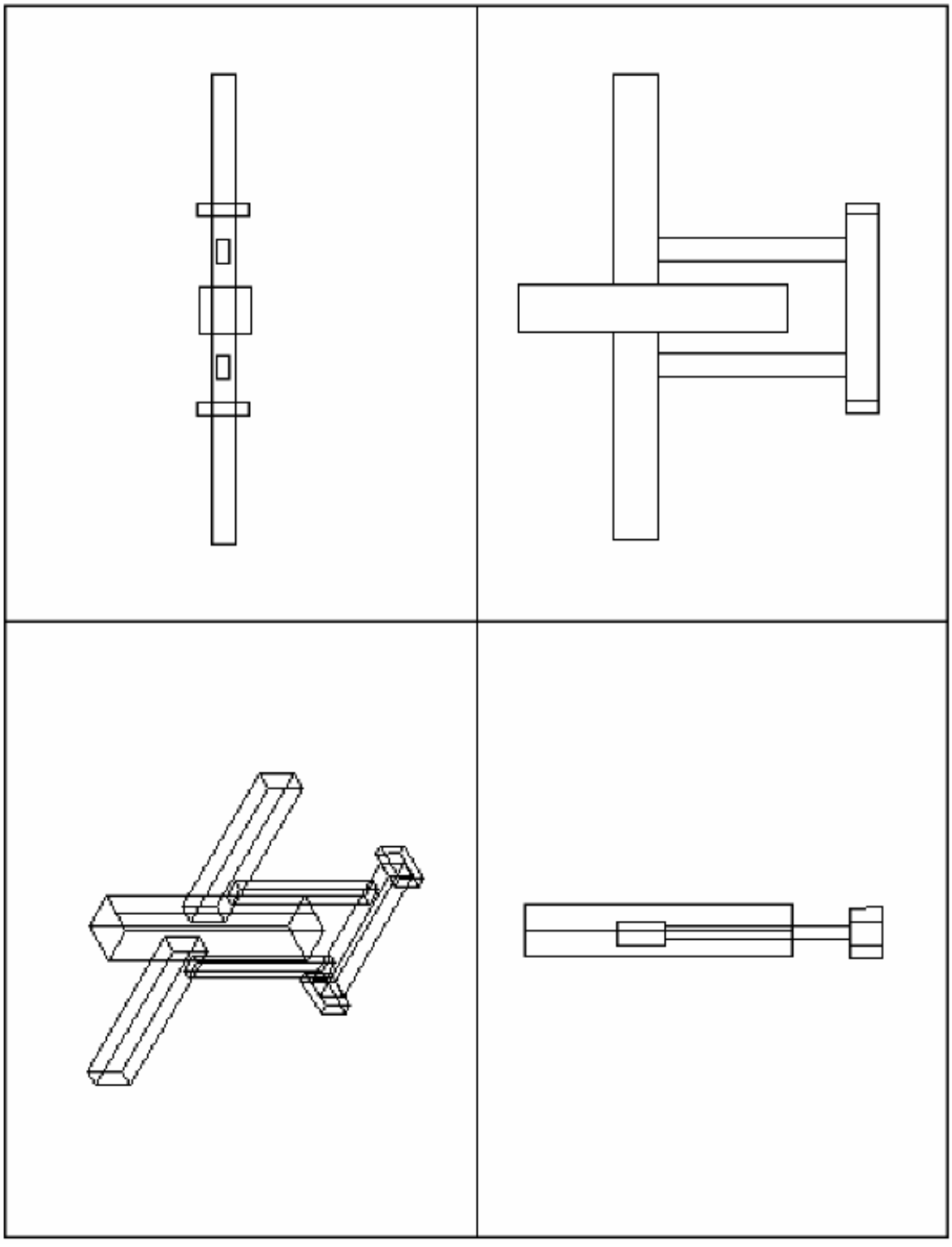

APPENDIX II
MAV DESIGN 2

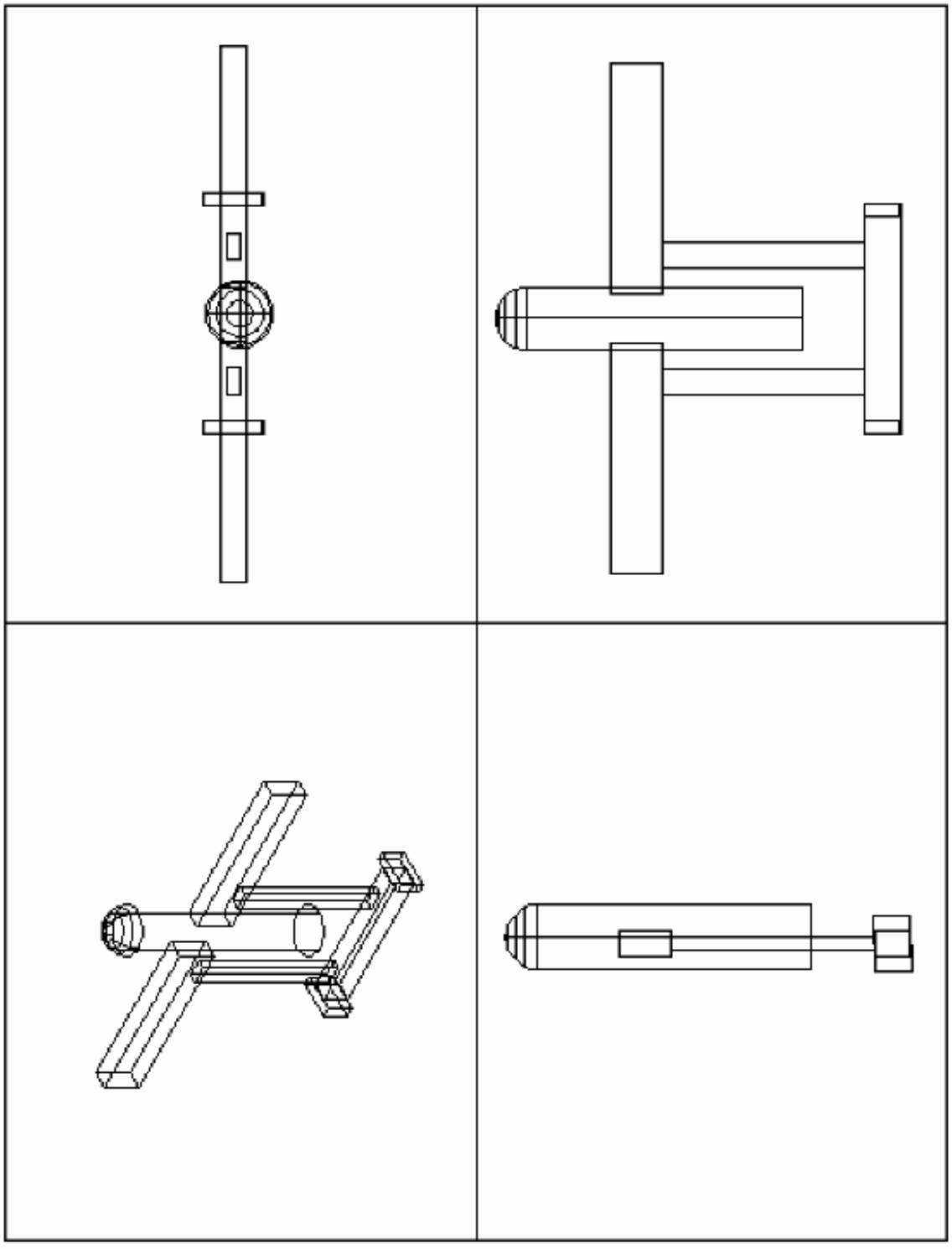

APPENDIX III
MAV DESIGN 3